N O T I C E

THIS DOCUMENT HAS BEEN REPRODUCED FROM MICROFICHE. ALTHOUGH IT IS RECOGNIZED THAT CERTAIN PORTIONS ARE ILLEGIBLE, IT IS BEING RELEASED IN THE INTEREST OF MAKING AVAILABLE AS MUCH INFORMATION AS POSSIBLE

NASA TECHNICAL MEMORANDUM

NASA TM-75694

NUMERICAL EXPERIMENTS ON THE THETA PINCH

P. R Volosevich, G.G. Zukakishvili, G.S. Latsabidze, Ye.I. Levanov, Yu.P. Popov, N.M. Skhirtladze, E.K. Tikhanov

Translation of "Chislennyye eksperimenty po teta-pinchu," Academy of Sciences USSR, Institute of Applied Mathematics imeni M.V. Keldysh, Moscow, Preprint No. 47, 1979, pp 1-30

NATIONAL AERONAUTICS AND SPACE ADMINISTRATION
WASHINGTON D.C. 20546
October 1979

NUMERICAL EXPERIMENTS ON THE THETA PINCH

P.P. Volosevich, G.G. Zukakishvili, G.S. Latsabidze, Ye.I. Levanov, Yu.P. Popov, N.N. Skhirtladze, E.K. Tikhanov
USSR Academy of Sciences, Keldysh Institute of Applied Mathematics, Moscow

1. Introduction

Theta pinch systems occupy an important place in studies of dense high temperature plasma. Here, detailed theoretical study of theta pinch, because of the necessity of taking account of many nonlinear processes (gas dynamic motion, magnetic field diffusion, Joule heating by temperature dependent conduction, electron and ion heat conductivity, bulk energy losses and other effects), is impossible without the use of numerical calculations by computer. /5

A two temperature nature is characteristic of theta pinches (and, generally, for fast, high current discharges). The ion component of the plasma in theta pinches is heated by rapid radial compression and subsequent slow final compression in a magnetic field which increases over time. The electron temperature changes, both due to compression, and as a result of Joule heating. Since the relaxation time between the electrons and ions, as a rule, is greater than or comparable with the characteristic time of the process, the plasma components can have different temperatures: $T_e \neq T_i$.

Experiments show [1-2] that "end" losses (escape of mass, impulse and energy through the ends of the plasma pinch) also can significantly affect the dynamics of the process in theta pinches.

To study a theta pinch with end losses, formulation of at least a two dimensional problem is necessary. However, for a qualitative analysis of the processes, it also is advisable to consider a one dimensional problem, which models the end losses, with bulk escape of mass, impulse and energy. /6

*Numbers in the margin indicate pagination in the foreign text.

Some results of numerical calculations of theta pinch problems are presented in this study. The physical processes in theta pinch systems are considered in a one dimensional two temperature magnetohydrodynamic approximation, with allowance for end losses by longitudinal heat conductivity. The numerical calculations are compared with experiments conducted earlier at SFTI [3]. The comparison gives satisfactory results for a number of parameters. However, there also are a number of disagreements of the results and experimental data. This makes further refinement of the physical and mathematical formulation of the problem necessary. The results of preliminary numerical calculations of the two meter theta pinch built at SFTI are presented.

2. Formulation of the Problem

Electrical capacitance C, with initial voltage U_0 on it, is discharged in a coil, a circular metal cylinder cut along the generatrix. The cylinder length is ℓ and the radius, r_*. A discharge chamber is placed inside the cylinder. It is filled with a hot, conducting deuterium plasma with initial temperature $T_e^0 = T_i^0$. It is assumed that the chamber walls are electrically nonconducting and that the conductivity in the annular region between the plasma and the coil (vacuum) is zero. We will consider the process of compression and heating the plasma pinch with a magnetic field, on the assumption of axial symmetry, in a two temperature magnetohydrodynamic approximation, with allowance for electron and ion heat conductivity, Joule heating and bulk energy losses. /7

The corresponding system of magnetohydrodynamic equations, with allowance for the effects listed above, in Lagrangian mass coordinates, has the form:

$$\frac{\partial}{\partial t}\left(\frac{1}{\rho}\right) = \frac{\partial}{\partial m}(rv), \quad \frac{\partial r}{\partial t} = v \tag{1}$$

$$\frac{\partial v}{\partial t} = -r\frac{\partial}{\partial m}(p_e + p_i) + f_r, \quad f_r = -r\frac{\partial}{\partial m}\left(\frac{H_\varphi^2}{8\pi}\right), \tag{2}$$

$$\frac{\partial \varepsilon_e}{\partial t} - p_e\frac{\partial}{\partial m}(rv) = -\frac{\partial W_e}{\partial m} + \frac{1}{\rho}Q_{ie} + \frac{\sigma E_\varphi^2}{\rho} + \frac{Q_e}{\rho} + \frac{1}{\rho}W_e' \tag{3}$$

$$\frac{\partial \varepsilon_i}{\partial t} - p_i\frac{\partial}{\partial m}(rv) = -\frac{1}{\rho}Q_{ie} - \frac{\partial W_i}{\partial m} \tag{4}$$

$$\frac{\partial}{\partial t}\left(\frac{H_\varphi}{\rho}\right) = -c\frac{\partial(rE_\varphi)}{\partial m} \tag{5}$$

$$dE_e = -P_e \frac{\partial z}{\partial m} - \frac{\partial W_e}{\partial m} \qquad (6)$$

$$W_e = -\varkappa_e z^2 \rho \frac{\partial T_e}{\partial r} \qquad (7)$$

$$W_i = -\varkappa_i z^2 \rho \frac{\partial T_i}{\partial r} \qquad (8)$$

Here, t is the time, r is the Euler coordinate, m($dm=\rho z dr$) is the Lagrangian mass coordinate, the Lagrangian time derivative, v is the plasma velocity, ρ is the density, ε_e; ε_i; T_e and T_i are the specific internal energy and temperature of the electrons and ions, respectively, P_e and P_i are the electron and ion pressure, W_e and W_i are the radial heat flows due to electron and ion heat conductivity, κ is the coefficient of heat conductivity, Q_{ie} is the electron-ion relaxation, Q_e is the intrinsic plasma bremsstrahlung, H_z and E_ϕ are the axial and azimuthal components of the magnetic field strength, respectively, σ is the conductivity and c is the velocity of light.

Functions W_z express the end losses of energy in the plasma pinch /8 by longitudinal (directed along the pinch axis) component of the electron heat conductivity flow. It is expressed by the quantity

$$W_z = -\varkappa \cdot \frac{T_e}{\ell} \qquad (9)$$

where $K=K(T_e)$ is the temperature dependent coefficient of heat conductivity and ℓ is the length of the plasma pinch.

We shall consider the quantities which express the physical properties of the deuterium plasma, or the assumption of complete ionization, with the use of the formulas presented in 4, 5 for their calculation:

$$\sigma = 1{,}03 \cdot 10^{14} \frac{T_e^{3/2}}{A} \frac{1}{\text{sec}} = 1{,}03 \cdot 10^{2} \frac{T_e^{3/2}}{A} \frac{1}{\text{ohm} \cdot \text{cm}} \qquad (10)$$

$$\varkappa_e = 1{,}3 \cdot 10^{6} \frac{T_e^{5/2}}{A\left(1 + 1{,}5 \cdot 10^{-6} \frac{T_e^{2}}{A \rho^{2/3}}\right)} \frac{\text{erg}}{\text{cm} \cdot \text{sec} \cdot \text{eV}} \qquad (11)$$

$$Q_{ie} = 1{,}8 \cdot 10^{-19} \frac{A \rho^{2}}{T_e^{3/2}} \frac{\text{erg}}{\text{cm}^3 \cdot \text{sec}} \qquad (12)$$

$$Q_e = 1{,}69 \cdot 10^{-32} \rho^{2} T_e^{1/2} \frac{\text{erg}}{\text{cm}^3 \cdot \text{sec}} \qquad (13)$$

$$\frac{\text{erg}}{\text{cm}\cdot\text{sec}\cdot\text{eV}} \tag{14}$$

$$\frac{\text{erg}}{\text{cm}\cdot\text{sec}\cdot\text{eV}} \tag{15}$$

In formulas (9)-(13), the quantity Λ is the Coulomb logarithm, the temperature is measured in electron volts, and the remaining quantitites, in the CGS system.

We will consider the equation of state of an ideal gas to be valid:

(16)

System of equations (1)-(14) is solved in the region $0< m< M(0<r<r_0)$, /9 where r_0 is the radius of the discharge chamber, M is the plasma mass in one radian, in units of length of the plasma pinch.

With $m=0(r=0)$, the symmetry conditions

$$v(0,t)=0,\quad W_e(0,t)=0,\quad W_i(0,t)=0,\quad E_\varphi(0,t)=0 \tag{17}$$

are assigned. With $m=M(r=r_0)$,

$$v(M,t)=0,\quad W_e(M,t)=0,\quad W_i(M,t)=0,\quad H_\varphi(M,t)=4\pi\frac{I(M,t)}{c} \tag{18}$$

where discharge current $I(M,t)$ is determined from the electric circuit equations

$$\frac{L}{c^2}\frac{dI}{dt}+RI+U=E_\varphi(M,t)=-4\pi^2\frac{\partial}{\partial m}\left[(r_1^2-r_0^2)\frac{\partial I}{\partial t}\right] \tag{19}$$

$$\frac{dU}{dt}=\frac{I}{C} \tag{20}$$

with the initial conditions

$$I(M,0)=0,\qquad U(M,0)=U_0 \tag{21}$$

Here, L, R and C are the inductance, resistance and capacitance in the external circuit, respectively, and U_0 is the initial voltage. The problem formulated above was solved, by means of difference methods developed at the Institute of Applied Mathematics, Academy of Sciences USSR, described in detail in [6-10]. We present some results of numerical solution of the problem formulated above.

3. Results of Numerical Experiments for "Small" Theta Pinch

A series of calculations was carried out for the so called "small" theta pinch system, which was studied experimentally at SFTI 3 . The initial parameters were as follows: electrical capacitance C=120μF, initial voltage U=33kV, ohmic resistance of circuit R=10^{-3} ohm, inductance /10
L=$7\cdot10^{-8}$ H. At the initial time t=0, it is assumed that the deuterium plasma is heated to temperature $T_e^0=T_i^0$=5eV, initial magnetic field H_z^0=0, chamber radius r_0=3.5 cm, initial density $\rho^0=2.34\cdot10^{-9}$ g/cm^3 ($n^0=7\cdot10^{14}$ cm^{-3}). The length of the plasma pinch along the z axis is ℓ=21cm.

The changes of the outer boundaries of the plasma pinch r and discharge current I in the circuit vs. time during a half period are shown in Fig. 1. After the first maximum compression, which is reached at t=0.3 μsec, some radial oscillations of the plasma are observed, which die out completely at time t=1.4 μsec. Current amplitude I=1.15MA, and the discharge half period T/2=10.5 μsec.

The average values of temperatures T_i and T_e and density ρ (averages over the entire plasma pinch mass M, i.e., $\bar{T}_i = \frac{1}{M}\int_0^M T_i\, dm$ etc.) vs. time and number of neutrons $N=2\cdot10^{16}\int_0^t\int_0^M \langle\sigma v\rangle_{dd}\, n\, dm\, dt$ at time t.

The maximum average temperatures are reached before the time of the discharge current maximum ($T_{emax}\approx$ 119eV), at t=4 μsec and $T_{imax}\approx$ 440eV, at t=2.2 μsec. This is connected primarily with the longitudinal electron heat conductivity and, to a somewhat lesser extent, with the transverse ion and electron heat conductivities. The maximum density ρ=$2.9\cdot10^{-7}$ g/cm^3 (ρ/ρ^0=124) is reached near the magnetic field maximum. The temperature and density fluctuations which arise in the initial stage of the process, just like the inertial oscillations of the plasma pinch (see Fig. 1), die out over time. There is a significant "breakaway" of the ion component of the temperature from the electron component, which /11
reaches the highest values at the time of the maximum of T_i. The basic source of heating of the ion component is the work of the compression forces of the plasma, with the increasing magnetic field. The ions exchange energy by collisions with electrons, part of which then is lost

from the system by longitudinal electron heat conductivity (see Eq. 3-4). After the T_i maximum, the rate of increase in the magnetic field is so small that the rate of escape of energy becomes greater than the rate of supply of energy (see Fig. 6). Therefore, toward the end of the half period, T_i relaxes to the value of T_e. The number of neutrons per discharge is the quantity $N=0.6\cdot10^5$ neutron/discharge.

Profiles of mass Lagrangian coordinate m as a function of temperature T_e (solid line), T_i (dashed line), density ρ (line with triangles) and magnetic field strength H_z (dot-dashed line) at various moments of time, indicated by the corresponding figures on the curves (time is presented in microseconds) are given in Fig. 3, 4. In the initial stage of the process, the magnetic field forms a skin near the outer boundary of the plasma. The azimuthal current density and Joule heating rate are at a maximum in this region. Because of this, the electron temperature is higher than the ion temperature on the surface of the plasma pinch and lower than T_i in the remaining part of the system. In time, the temperature equalizes quite rapidly over the mass of the pinch, and we have $T_i>T_e$ everywhere. The radial distribution of the shock wave and its accumulation on the pinch axis are followed from the density profiles. After the inertial oscillations of the plasma die out, the density distribution has a bell shape.

The energy values which make up the balance of the total energy of the system vs. time are presented in Fig. 5:

$$\mathcal{E}+V+W+\alpha+\beta+Q_4-\mathcal{E}^0-\beta^0-Q_2-\bar{Q}_0=0 \qquad (22)$$

Here, $\mathcal{E}=\int \frac{\varepsilon}{2}U^2$ electromagnetic energy in capacitance; /12

$\alpha=0.5\frac{L}{2}\mathcal{J}^2$ energy in inductance;

$Q_C=\int_0^t \frac{R}{2}\mathcal{J}^2 dt$ energy converted to Joule heat of external resistance (circuit losses);

$W=\int_0^{m_k} \frac{H_z^2}{8\pi}dm$
$V=\int_0^{m_k} \frac{u^2}{2}dm$
$\mathcal{E}=\int_0^{m_k}(\mathcal{E}_e+\mathcal{E}_i)dm$

magnetic field energy, kinetic energy and total internal energy of system, respectively, at given time;

energy losses by longitudinal electron heat conductivity and due to plasma bremsstrahlung;

β^0 and ε^0 initial circuit electromagnetic energy and plasma internal energy.

It follows from the calculations that the efficiency of conversion of the electrical energy of the external circuit to internal energy, as a function of the initial conditions, is in the 0.0014-0.009 range. The energy losses due to longitudinal heat conductivity turn out to be comparable to the internal energy, while the energy losses due to bremsstrahlung of a pure deuterium plasma do not play a significant part in the energy balance. The energy values which make up the internal energy balance of the system vs. time are presented in Fig. 6:

(23)

here, $A = -\int_0^t \int_0^M (p_e + p_i) \frac{\partial}{\partial m}(\pi r^2 v)\, dm\, dt$ work of compression; /13

$Q_J = \int_0^t \int_0^M \sigma E_\varphi^2 / \rho \, dm\, dt$

Joule heat of system.

It is evident that the work of compression plays a considerably greater part than Joule heat.

Fig. 7 and Table 1 illustrate the effect of longitudinal electron (W_z) and radial ion (W_i) heat conductivity on the processes under consideration. The average ion temperature vs. time for various versions of the calculation is presented in Fig. 7. The case $W_z \neq 0$, $W_i \neq 0$ is plotted as a solid line, $W_z \equiv 0$, $W_i \equiv 0$, as a dashed line, $W_z \equiv 0$, $W_i \neq 0$, as a dot-dash line and $W_z = 0$, $W_i \equiv 0$, as a dash-double tick line. The maximum plasma temperature and density, the number of neutrons per discharge and the energy conversion efficiency for the abovementioned versions of the calculations are presented in Table 1. It is evident that both current W_z and current W_i significantly affect the plasma parameters. However, the energy losses by longitudinal heat conductivity play a decisive role. Allowance for W_z leads to a considerable reduction in the ion and electron temperatures. The efficiency of conversion of electromagnetic energy to internal plasma energy is reduced to half, in

this case. Here, the plasma concentration changes comparatively little. The most sensitive parameter is the neutron yield, which, depending on the calculation conditions, changes by three orders of magnitude. Currents W_2 and W_1 affect both the amplitude of the quantities and, also, these quantities vs. time (see Fig. 7).

TABLE 1.

Quantities \ Calculation version	$W_2' \neq 0$, $W_1' \neq 0$	$W_2' \neq 0$, $W_1' = 0$	$W_2' = 0$, $W_1' \neq 0$	$W_2' = 0$, $W_1' = 0$
T_i (eV)	441	538	717	835
T_e (eV)	II9	II2	I008	903
ρ_{max}	I24	III	76	75,5
N neutron discharge	$0.6 \cdot I0^5$	$3.4 \cdot I0^6$	$2.5 \cdot I0^6$	$I.3 \cdot I0^7$
$\frac{\mathcal{E}+V}{\beta}$	0.00I4	0.00I54	0.0035	0.0037
t at T_i max (10^{-6} sec)	2.2	2.42	5.27	5.27

4. Comparison with Experiment

Comparison of the calculations carried out for the "small" system, /16 with allowance for the longitudinal electron and transverse ion heat conductivities, with the experimental results [3] shows that there is quantitative coincidence of the parameters (Table 2). This model describes well the electrical engineering parameters of the discharge circuit (I, T) and the initial stage of the process, including the rapid compression and subsequent inertial plasma oscillations. The calculated and measured electron temperatures are consistent.

At the same time, significantly understated ion temperatures T_i and neutron yields and overstated plasma concentrations were obtained in the calculations. It does not correspond to experience at the stage of slow, adiabatic final compression of the plasma and time changes of the plasma pinch radius r, T_i and N.

In the experiment, r decreases monotonically, and T_i and N reach maximum values in the magnetic field maximum. In the calculations, r is practically constant over time, but T_i and N reach maximum values in the first quarter of the period. The cause of this discrepancy may be particle losses through the ends of the system. The most severe end losses should show up in short pinches. Qualitative analysis shows that the escape of mass may result in additional heating of the particles remaining in the system, due to the adiabatic final compression of the plasma.

TABLE 2.

	n^0 [cm^{-3}]	T discharge period [10^{-6} sec]	current J [MA]	1st oscillation time [10^{-6} sec]	n_{max} [cm^{-3}]	T_e [eV]	T_i [eV]	neutron discharge
Theory	$7\cdot10^{14}$	21	1.15	0.3	$8.5\cdot10^{16}$	119	440	$0.6\cdot10^5$
Experiment	$7\cdot10^{14}$	19±0.5	1.3±0.15	0.3±0.05	$2\cdot10^{16}$ ± $1.1\cdot10^{16}$	100±20	1200±200	$7\cdot10^5$±$2\cdot10^5$

5. Results of Numerical Experiments for Two Meter Theta Pinch

Similar calculations were carried out for the two meter theta pinch built at SFTI (ℓ=200 cm), experiments on which will start in the second half of 1979. The inital data were the following: C = 1920μF, U_0 = 35kV, R = $3\cdot10^{-5}$ohm, L = $8.5\cdot10^{-9}$H, $T_e^0 = T_i^0$ = 5eV. /17

The average electron and ion temperatures and concentrations vs. time, as well as the total number of neutrons at time t, for initial density $\rho^0=2.34\cdot10^{-9}$g/cm^3 ($n^0=7\cdot10^{14}$cm^{-3}), are presented in Fig. 8. Version (1) corresponds to the case, when there is no escape of heat by longitudinal electron heat conductivity (W_z=0). In version (2), the coefficient of longitudinal electron heat conductivity for a deuterium plasma is used (z=1). Allowance for longitudinal electron heat conductivity reduces the value of T_e from 1900eV to 470eV. A comparison of the calculation results for the "small" (see Fig. 2) and "large" systems shows that a tenfold increase in pinch length ℓ results in a 3-4 times increase of T_e (this result is consistent with the approximate analytical relationship $T_e \sim \sqrt{\ell}$, obtained from analysis of the energy balance of the

electron component of the plasma). The electron temperature reaches the maximum value in the initial stage of the discharge, and it subsequently changes little.

A series of studies [11, 12] in recent years has been devoted to study of a method of limitation of end losses, by means of physical plugs (closures). Physical closures on the ends of the theta pinch should both exclude losses of particles from the plasma, and reduce (limit) energy losses caused by longitudinal electron heat conductivity, by the formation of a high z plasma in the area of the plugs ($\alpha_{//} \sim \frac{1 + 0{,}59\, z^{-1}}{1 + 0{,}28\, z + 0{,}31 z^2} = 1$ [5]). The value of z should be selected, so that radiation losses do not exceed losses by longitudinal electron heat conductivity. Estimates show that, at the optimum z=30, coefficient /18
$\kappa_{\parallel}$ decreases approximately eightfold. Numerical calculations for z=20 (Fig. 8(3)) give an appreciable increase in electron temperature over the z=1 case (this result should be considered approximate, since it was obtained within the scope of a one dimensional mathematical model with bulk discharges).

The maximum ion temperature depends little on $\kappa_{\parallel}$. Since the relaxation time τ_{ei} is comparable to the half period T/2, a considerable gap is retained between T_e and T_i, during the entire half period.

The radial distributions of functions ρ, T_e, T_i, H_z and j, for time t=7.1 sec, with initial density $\rho^0 = 2.34 \cdot 10^{-9}$ g/cm^3, are presented in Figs. 9 and 10. With $\kappa_{\parallel} = 0$ (Fig. 9), an electron temperature peak forms at the boundary of the plasma pinch (T layer [13]). Inclusion of the longitudinal electron heat conductivity corresponding to z=1 results in resorption of the T layer (Fig. 10).

The authors thank A.A. Samarskiy, R.G. Salukvadze and S.P. Kurdyumov for interest in the work and useful discussions, as well as L.N. Busurina, for participation in programing, conduct of the calculations and processing of the results.

REFERENCES

1. Spalding, I.T., Nucl. Fusion 8, 161 (1968). /19

2. Green, T.S. et al, Phys. Fluids 10/8, 1663 (1971).

3. Kvartskhava, I.F., G.G. Zukakishvili, Yu.V. Matveyev, Yu.S. Gvaladze, N.A. Razmadze, A.A. Beshaposhnikov, E.K. Tikhanov, Z.D. Chkuaseli and E.Yu. Khautiyev, "Plasma heating and stability in a combination pinch," Doklad na Mezhdunarodnoy konferentsii po UTS i fizike plazmy. Medison, 1971. Reports to International Conference on UTS and Plasma Physics, Madison, 1971 , IAEA, 28/B-1.

4. Spitzer, L., Fizika polnost'yu ionizovannogo gaza [Physics of a Completely Ionized Gas], Foreign Literature Publishing House, Moscow, 1957.

5. D'yachenko, V.F. and V.S. Imshennik, "Magnetohydrodynamic theory of the pinch effect in a high temperature plasma," Voprosy teorii plazmy [Questions of Plasma Theory], Atomizdat Press, Moscow, issue 5, 1967, pp. 394-439.

6. Zel'dovich, Ya.B. and Yu.P. Rayzer, Fizika udarnykh voln i vysokotemperaturnykh gidrodinamicheskikh yavleniy [Physics of Shock Waves and High Temperature Hydrodynamic Phenomena], Nauka Press, Moscow, 1966.

7. Samarskiy, A.A., P.P. Volosevich, M.I. Volchinskaya and S.P. Kurdyumov, Zhurnal Vychislitel'noy matem, i matem. fiziki 8, 1025 (1968).

8. Popov, Yu.P. and A.A. Samarskiy, Zhurnal Vychislitel'noy matem. i matem fiziki 9, 953 (1969).

9. Gol'din, V.Ya., D.A. Gol'dina et al, "Study of problems of computer calculation of magnetic radiation hydrodynamics," Preprint Pr-36, Institute of Applied Mathematics, USSR Academy of Sciences, 1971.

10. Samarskiy, A.A. and Yu. P. Popov, Raznostnyye skhemy gazovoy dinamiki [Difference Schemes of Gas Dynamics], Nauka Press, Moscow, 1975.

11. Malone, R.C. and R.L. Morse, Phys. Rev. Letters 39/3, 134-317 (1977).

12. Commisso, R.I. C.A. Ekdahl, K.B. Freese, K.F. McKenna and W.E. Quinn, Ibid., 137-139.

13. Tikhonov, A.N., A.A. Samarskiy, L.A. Zaklyaz'minskiy, P.P. Volosevich, /20 L.M. Degtyarev, S.P. Kurdyumov, Yu.P. Popov, V.S. Sokolov and A.P. Favorskiy, DAN SSSR 173/4, (1967).

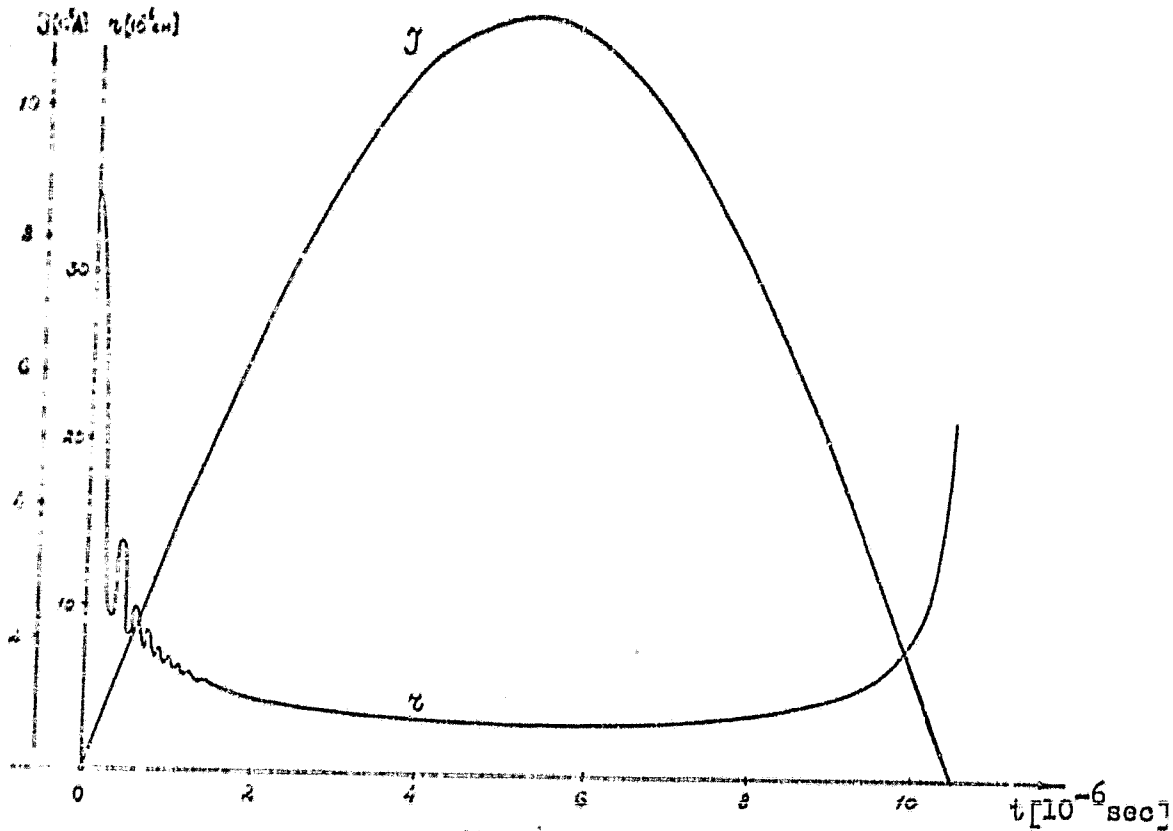

Fig. 1

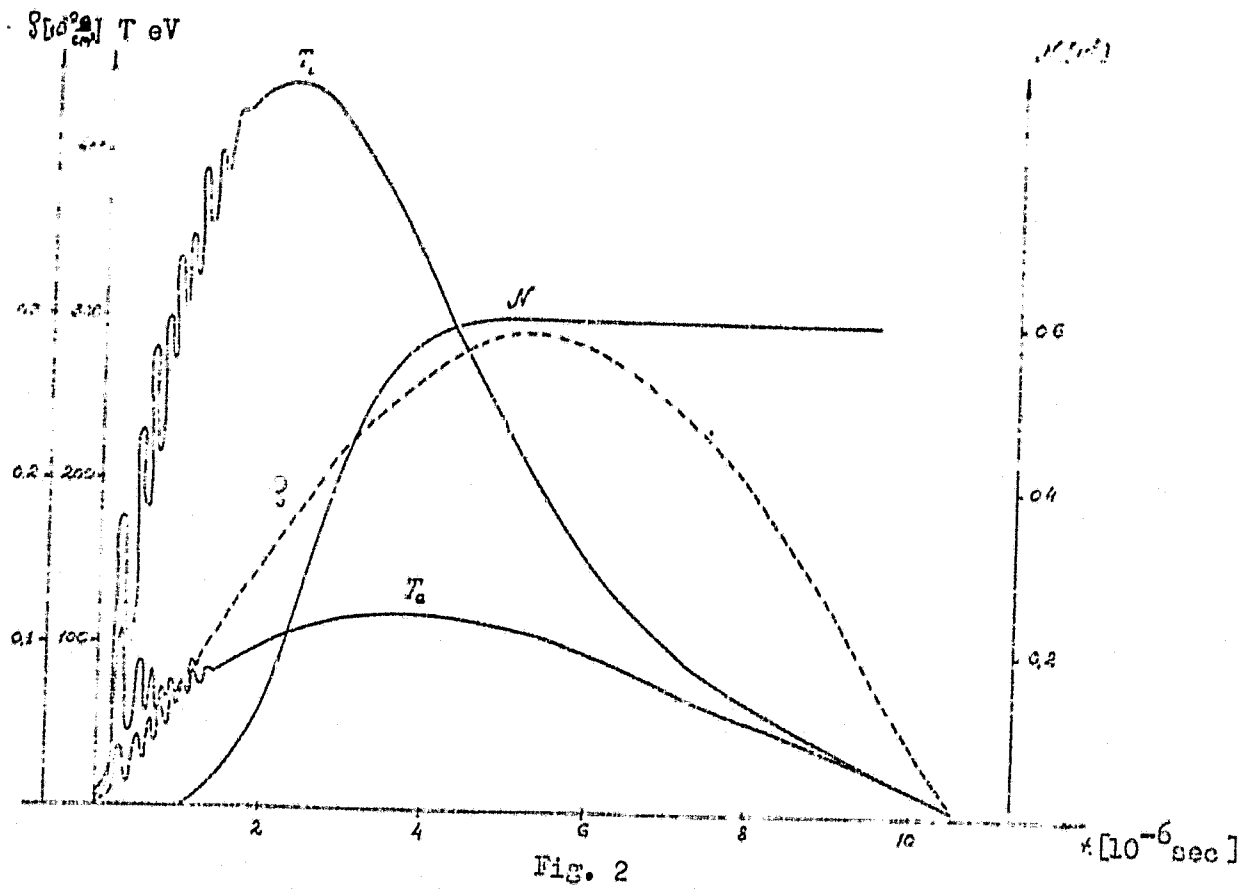

Fig. 2

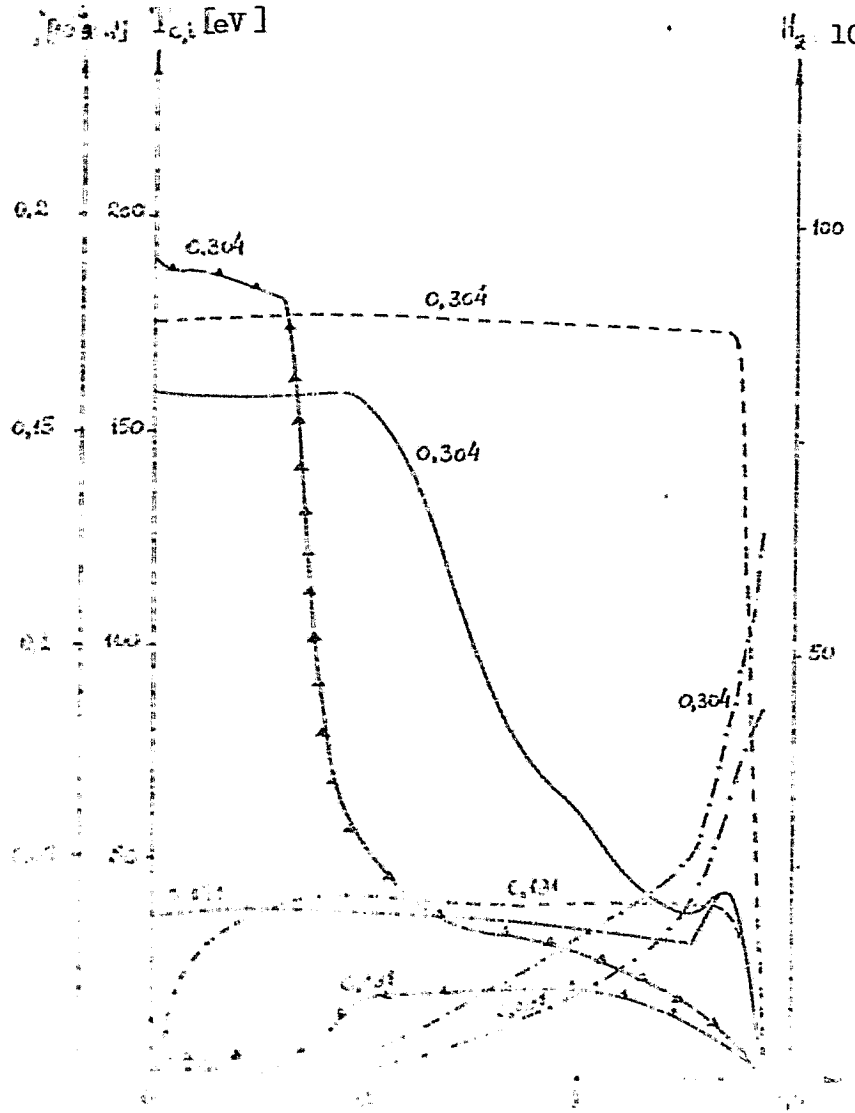
$T_{e,i}$ [eV]
H_z 10^2Oe
0,2
0,15
0,1
200
150
100
50
0,304
0,304
0,304
0,304
0,304
$m\,[10^{-8}\frac{g}{cm\cdot rad}]$

Fig. 3

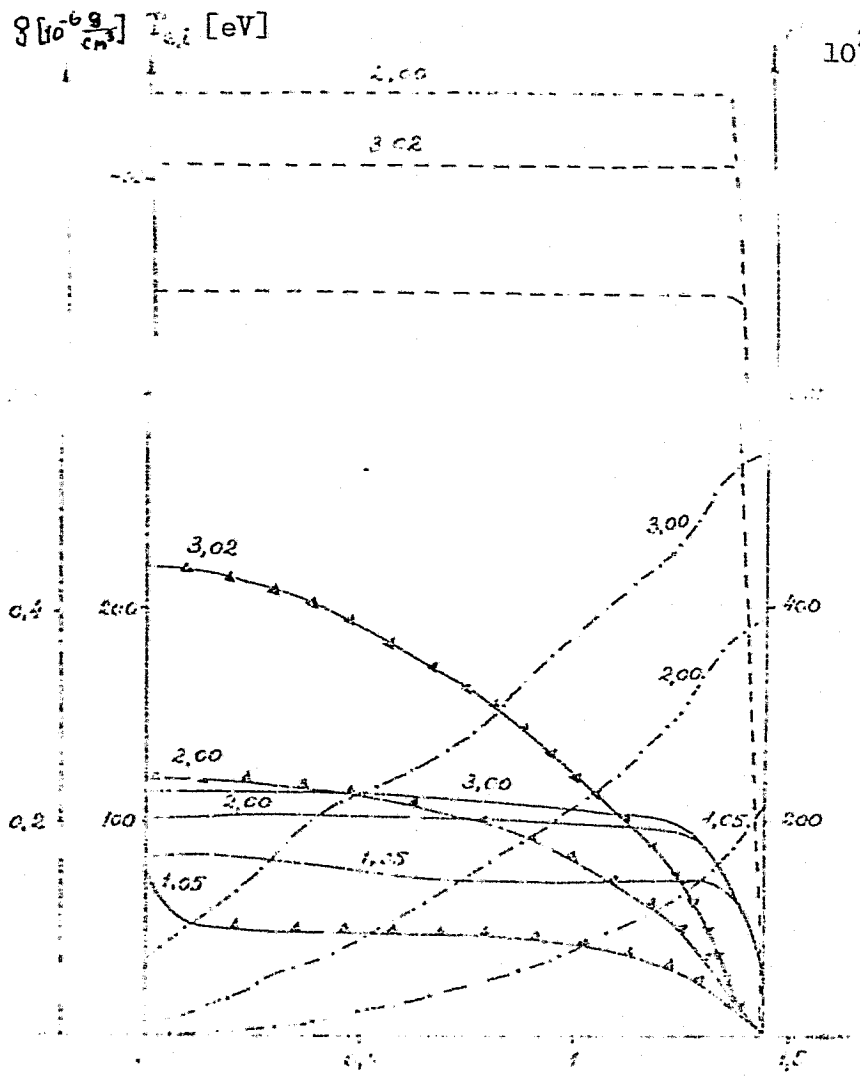
$\rho\,[10^{-6}\frac{g}{cm^3}]$
$T_{e,i}$ [eV]
10^2Oe
3,02
3,00
2,00
2,00
2,00
3,00
2,00
1,05
1,05
1,05
0,4
0,2
200
100
400
200
$m\,[10^{-8}\frac{g}{cm\cdot rad}]$

Fig. 4

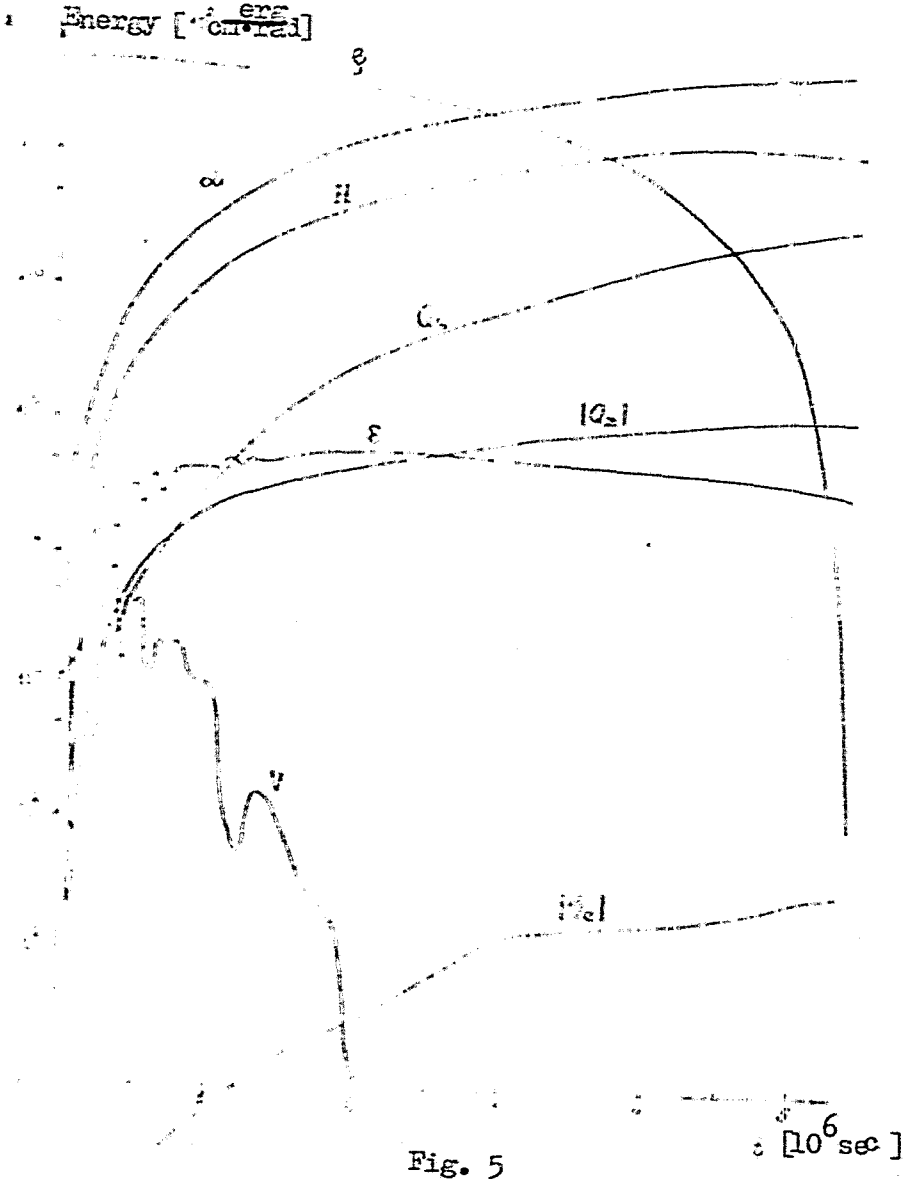
Energy [erg/cm·rad]
ℰ
α
H
ε
|Q_z|
|P_z|
[10^6 sec]

Fig. 5

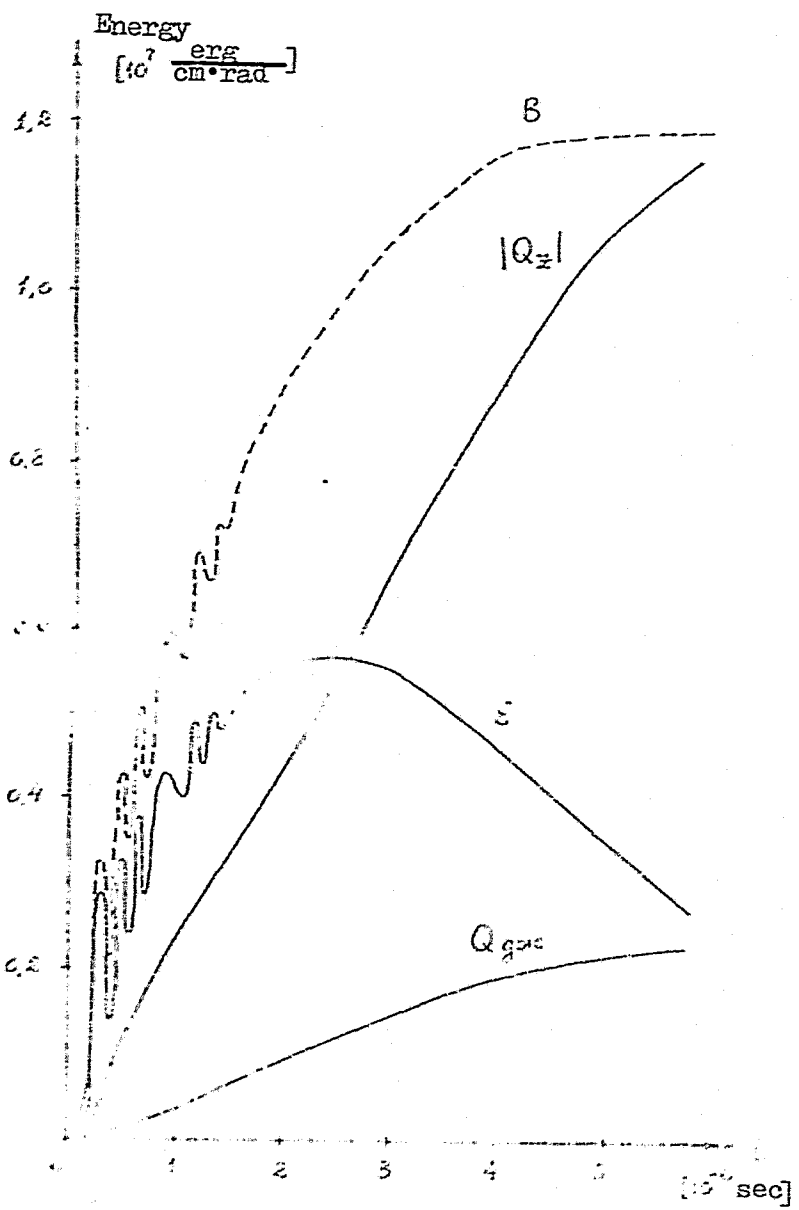
Energy
[10^7 erg/cm·rad]
1,2
1,0
0,8
0,4
0,2
B
|Q_z|
ε
Q_grav
1
2
3
4
5
[10^6 sec]

Fig. 6

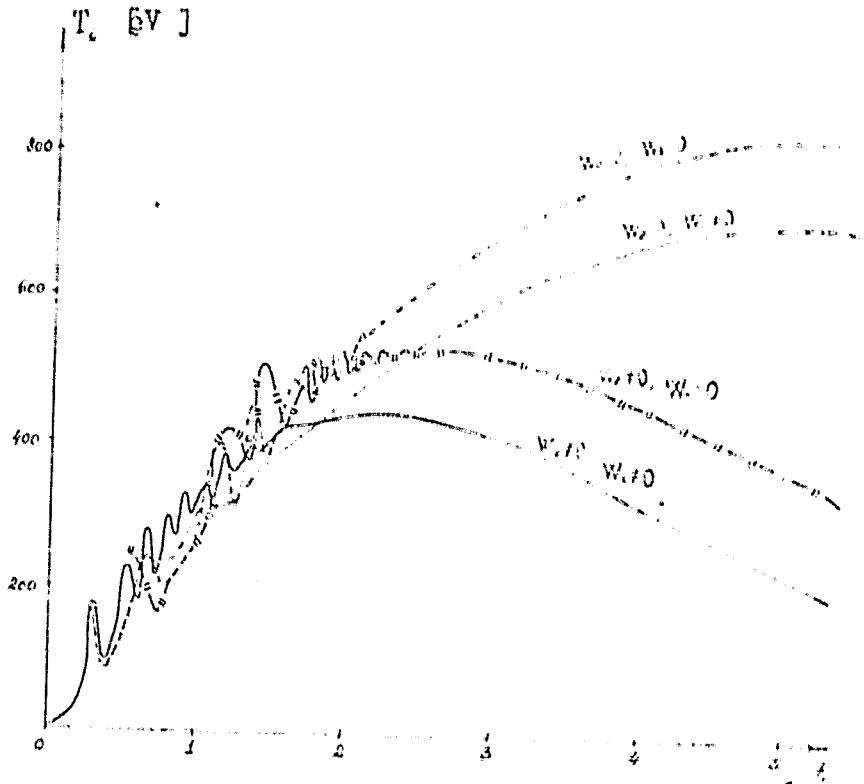
T_e [eV]
800
600
400
200
0
1
2
3
4
5
6
[10^6 sec]

Fig. 7

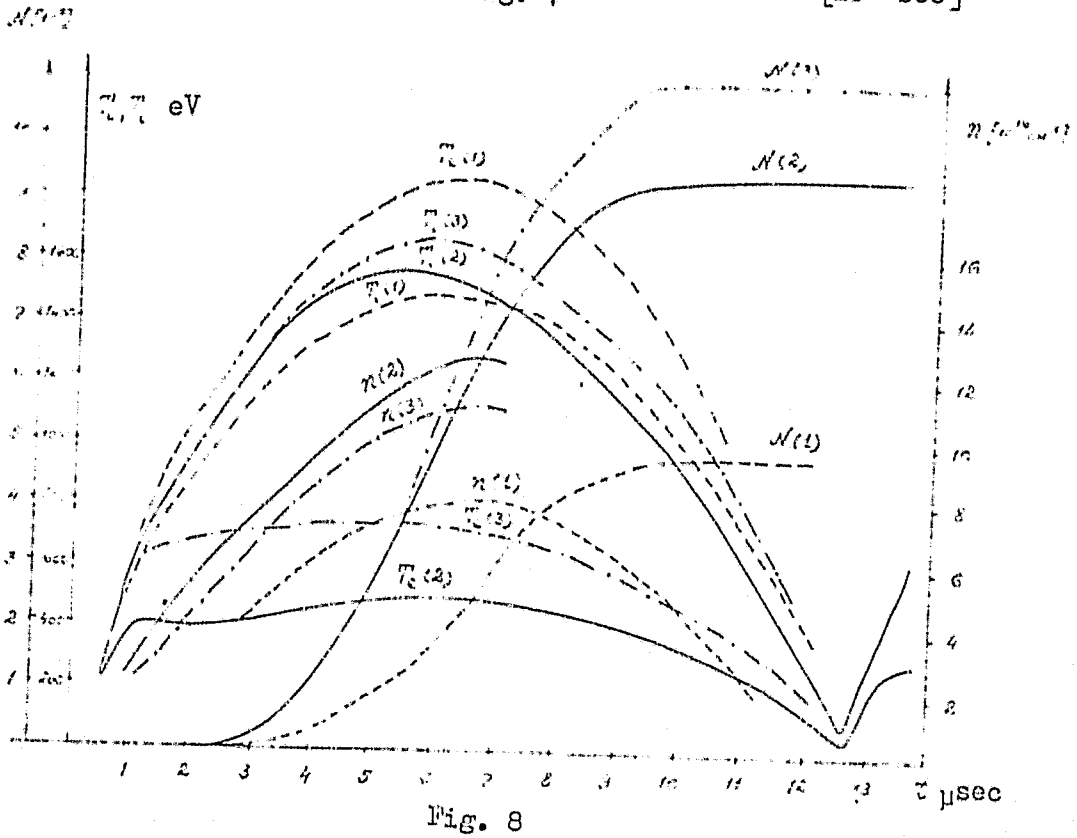
T_e, T_i eV
N(2)
N(1)
n(2)
n(1)
T_e(1)
T_e(2)
T_e(3)
T_i(1)
T_i(2)
T_i(3)
1
2
3
4
5
6
7
8
9
10
11
12
13
τ μsec

Fig. 8

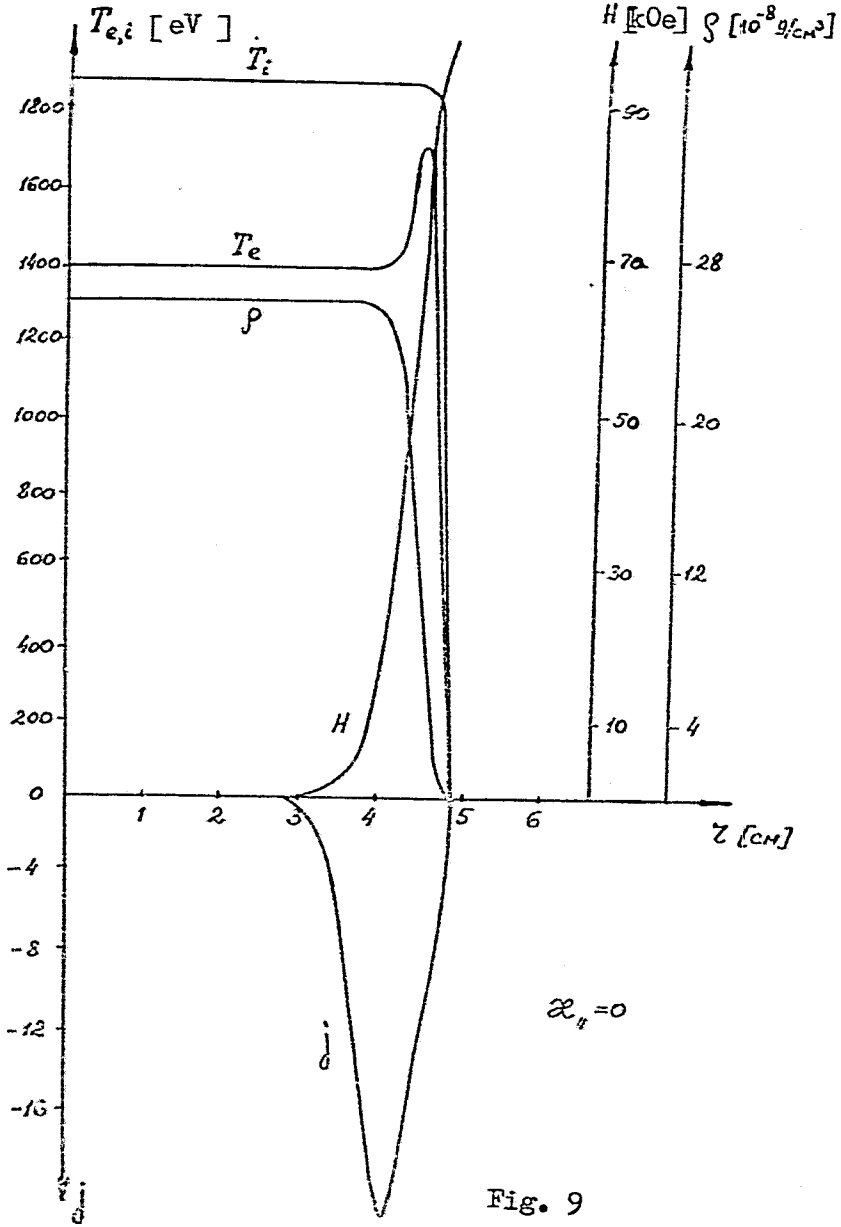
$T_{e,i}$ [eV]
T_i
T_e
ρ
H
j
H [kOe]
ρ [10^{-8} g/cm^3]
z [cm]
$\mathcal{H}_\parallel = 0$

Fig. 9

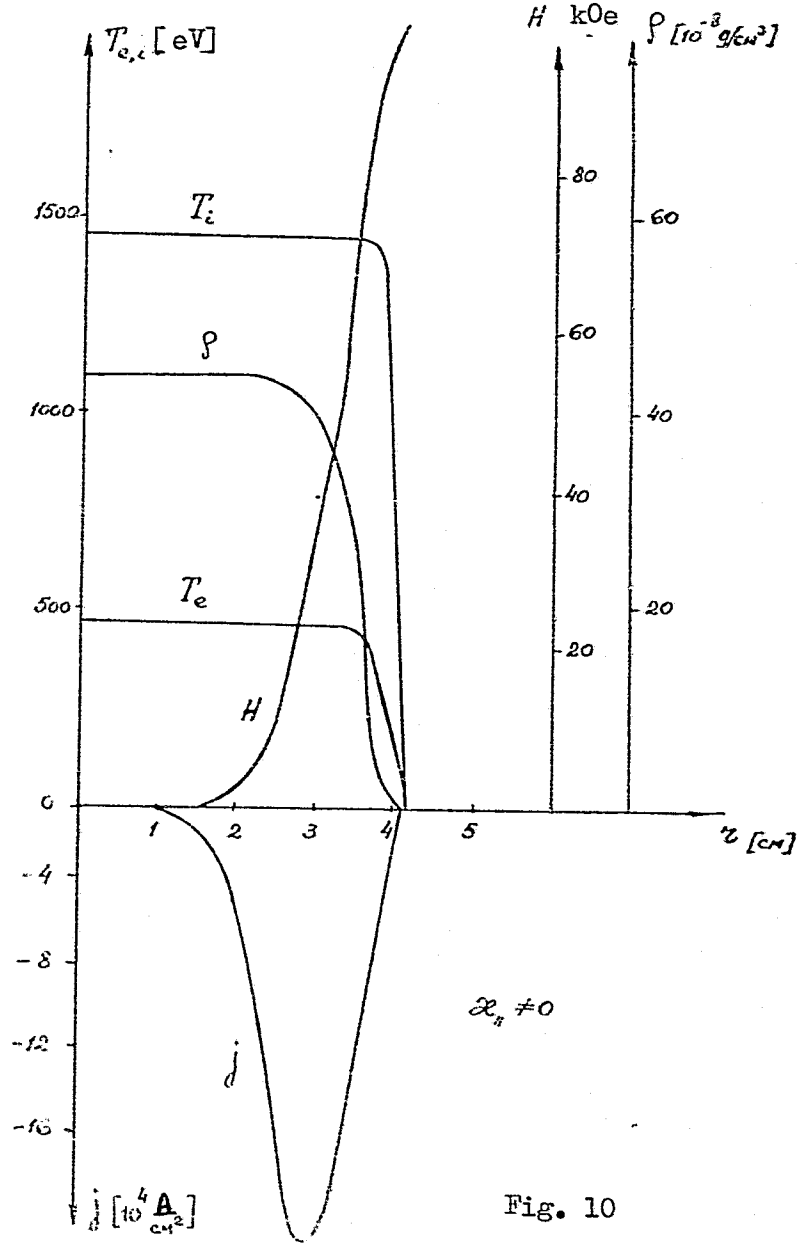
$T_{e,i}$ [eV]
T_i
T_e
ρ
H
j
H kOe
ρ [10^{-8} g/cm^3]
z [cm]
$\mathcal{H}_\parallel \neq 0$
j [10^4 A/cm^2]

Fig. 10